Indian Journal of Pure & Applied Physics
Vol. 61, December 2023, pp. 967-975
DOI: 10.56042/ijpap.v61i12.905

Simulation and Characterization of Optical Cavity for Iodine Stabilized Helium Neon Laser

Anju[a,b*], Girija Moona[a,b], Mukesh Jewariya[a,b], Poonam Arora[a,b] & Rina Sharma[a,b]

[a]CSIR-National Physical Laboratory, Dr. K. S. Krishnan Marg, New Delhi 110 012, India
[b]Academy of Scientific and Innovative Research (AcSIR), Ghaziabad 201 002, India

Received 26 April 2023; accepted 30 October 2023

Laser cavity design and characterization plays a crucial role in spectroscopy and development of wavelength standards. Frequency stability of laser is significantly affected by perturbations in environment effects on mirror mounts and fabrication quality of guide ways & mounts. While designing the laser resonator for iodine stabilized helium-neon (He-Ne) laser, linear mechanism of mirror mount is required to vary the cavity length, in order to scan the frequency for spectroscopy. In this investigation, we have designed a shaft consist of straight splines that will be used for the holding and linear movement of the mirror. This manuscript present the design of cavity for a He-Ne laser intended for intracavity spectroscopy of iodine, as well as simulation in octave software for stability analysis, and discussed the dimensional characterization of invar guide ways and spline shaft. Roundness of invar rods used area was measured using form tester (RA- 2200 CNC) and a coordinate measuring machine (3D-CMM, LEGEX 9106) was used for dimensional characterization of spline shaft, and the associated uncertainty of measurement was evaluated as per ISO GUM/LPU approach according to JCGM 100:2008.

Keywords: CMM; Design; Laser Resonator; Roundness; Spline Shaft; Uncertainty; Octave

1 Introduction

Laser head is constituted of laser resonator, gain medium in the resonator and pumping source for activating the gain medium. The gain medium is chosen as per the desired wavelength (lasing frequency). The cavity or resonator is designed keeping in mind single-mode/multi-mode laser operation where frequency of the laser can be tuned by tuning the length of cavity. This feature is utilized in high-resolution spectroscopy and development of frequency stabilized lasers. Laser cavity (LC) is the heart of laser system that comprises of two parallelly mounted mirrors separated by a space in which the laser gain medium is placed. This forms a Fabry Perrot interferometer. In a laser resonator, standing waves/longitudinal modes are formed by multiple reflections and wavelengths having half wavelength integral number fit in the cavity length, are sustained. Laser can operate in a single-mode/multi-mode operation depending on cavity length. Further, the resonator is a stable/unstable structure depending on parameters like radius of curvature, reflectivity of mirrors and length of cavity[1-3]. These parameters are to be optimized while designing the cavity or resonator. Laser light has a very high degree of mono-chromaticity[4]. However, this mono-chromaticity of frequency stability needs further enhancement for applications like precision spectroscopy and interferometry[5–8]. For example, i.e. a He-Ne laser has frequency stability of the order of 10^{-6}; this can be improved by frequency stabilization. The laser frequency can be tuned by changing the cavity length through displacement of the mirror. This feature is utilized in high-resolution spectroscopy and development of frequency stabilized lasers. Various methods that are used for frequency stabilization involve change in cavity length and locking the length to a frequency reference or a feature. A relative frequency stability of 10^{-8} to 10^{-9} can be achieved by two-mode stabilization or Zeeman stabilization[9,10]. Hyperfine transitions, used as a reference for locking the laser line using Doppler free spectroscopy and result in frequency stability of the order of 10^{-1111}. Iodine stabilized He-Ne laser act as a primary standard as per recommendation by CIPM (International Committee for Weights and Measures) for the practical realization of SI unit 'metre'. Iodine $^{127}I_2$ is recommended in the list of recommended standard frequencies as per CIPM[12].

*Corresponding author:
(E-mail: anju.narwana6@gmail.com)

The frequency stability of a laser is influenced by environmental impacts on mirror mounts and the manufacturing quality of guide ways and mounts. If the temperature changes, the material of the components can expand or contract, causing the misalignment. For laser measurements, a temperature-controlled environment is required. External vibrations should also be avoided in the laser system since they can cause the cavity mirrors to misalign. For high-precision applications, an anti-vibration optical table is preferred. Furthermore, humidity may affect the dielectric coating of the mirrors, reducing their reflectivity. As a result, humidity should be controlled as well. Likewise, dust particles can deposit on the optical components, causing light absorbance or scattering, resulting in a change in beam quality and degraded laser system performance. Hence, for high-precision applications, environmental conditions such as controlled temperature and humidity, as well as minimal vibrations, are essential for the mechanical stability of the cavity components and the system's reliable performance. Therefore, it is critical to conduct the dimensional characterization and measurement uncertainty evaluation of each cavity component. Every measurement result is complete only when it includes an estimate of the quantity being measured as well as a quantitative assessment of the reliability of that estimate. The present paper reports design of optical cavity and characterization of fabricated parts to be used in $^{127}I_2$ stabilized He-Ne Laser. Simulation studies have been carried out to achieve stable resonator with defined mirror and cavity parameters. Measurements are performed for the dimensional characterization of spline shaft and LC rod, designed for holding and translation of mirror and the uncertainty in measurements is evaluated using the internationally accepted Guide to the expression of uncertainty in measurement (GUM) document[13-17]. A traceable 3D-coordinate measuring machine (3D-CMM, LEGEX 9106) has been used for dimensional characterization of spline shaft. For measurement of roundness of LC rod; form tester (RA- 2200 CNC) has been used.

2 Simulation Studies

The mirrors employed for laser resonator are dielectric mirrors, designed with reflectivities of 99.9% and 99.5%. For measurement of reflectivity of mirrors, a He-Ne laser and power detector are used. Laser light is passed through the mirror and power of incident and transmitted beams are measured. While evaluating the reflectivity of mirrors, absorption by mirror is assumed to be negligible. The schematic of the set-up is shown in Fig. 1. The incident beam power is first measured by placing the probe in front of the dielectric mirror, following which the transmitted beam power is measured by positioning the probe behind the mirror. The transmittance coefficient was determined by considering the ratio of transmitted and incident beam power. Using this, reflectivity of the mirror was calculated through the formula R+T+A=1. R, T and A corresponds to the reflectance, transmittance and absorbance of the light. The corresponding observations are illustrated in Table 1.

The first step in designing the cavity was to estimate the length depending on single-mode laser operation, size of components to be placed in the cavity and estimated length was 320 mm. To check the appropriateness of the selected length and other parameters like radius of curvature of mirrors, we have carried out the simulation using octave software.

For simulation, the electric field needed to be discretized, since the computer could not analyze the continuous electric fields. Initially, the parameters of cavity are defined such as length of the cavity, mirrors

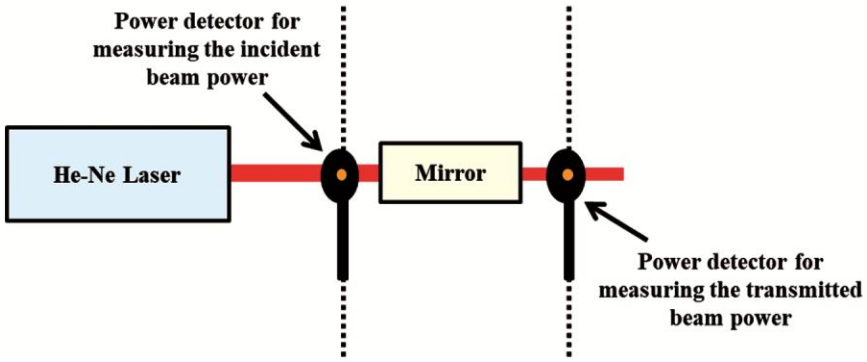

Fig.1 — Schematic for measurement of reflectivity of mirrors.

Table 1 — Observations for reflectivity measurement

S.No.	Incident beam power p_1(mW)		Transmitted beam power p_2(μW)		$(p_2/p_1) \times 10^{-3}$		Reflectivity (%)	
	M_1	M_2	M_1	M_2	M_1	M_2	R_{M1}	R_{M2}
1.	0.431	0.431	1.504	2.340	3.49	5.43	99.6	99.5
2.	0.429	0.431	1.489	2.320	3.47	5.38	99.6	99.5
3.	0.432	0.428	1.478	2.460	3.42	5.75	99.7	99.4
4.	0.431	0.429	1.481	2.380	3.44	5.55	99.7	99.4
5.	0.433	0.430	1.486	2.290	3.43	5.33	99.7	99.5
			Mean				99.7	99.5
			Standard Uncertainty				± 0.05	± 0.05

The experimental observations exhibit the reflectivity of 99.7 % and 99.5 % for the mirrors M_1& M_2 with a standard uncertainty of ± 0.05 %

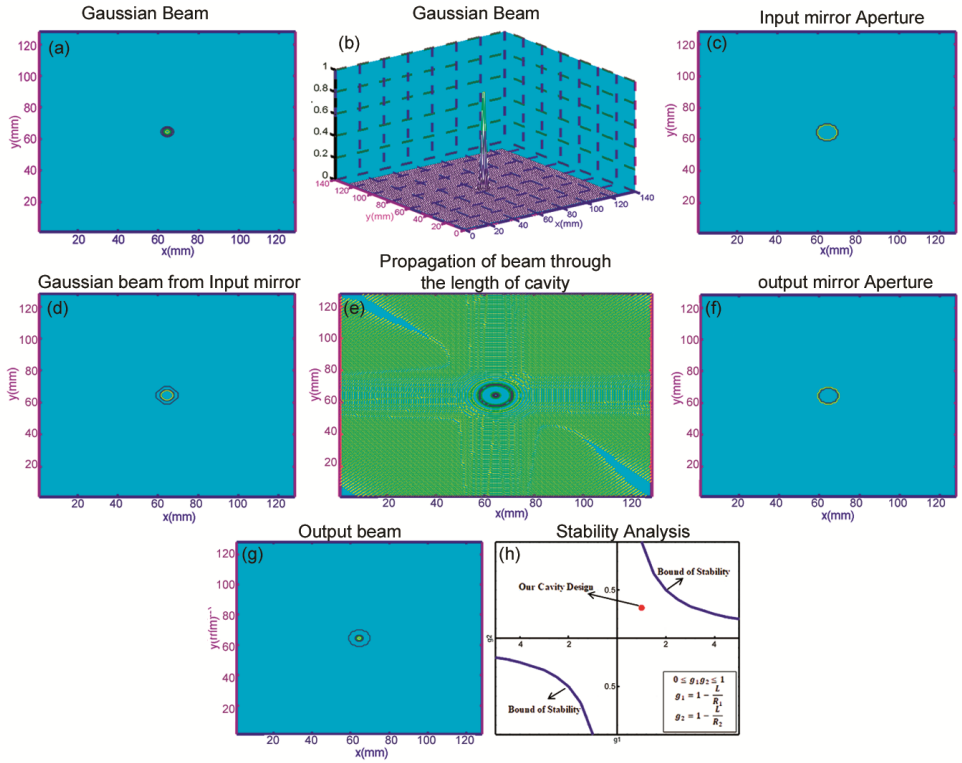

Fig. 2 — (a) Contour plot of the Gaussian beam (b) 3-D Gaussian beam profile (c) Input mirror aperture (d) Gaussian beam after passing through input mirror (e) Beam propagation through the length of the cavity (f) Output mirror aperture (g) Output beam (h) Stability analysis.

diameters, radii of curvature of mirrors, reflectivities of the mirrors, input laser beam wavelength, beam radius and optical power of the beam. After defining all the parameters, the Gaussian beam was discretized using electric field variation $E = E_0\, e^{-r^2/{w_0}^2}$. Where, r,$w_0$ and E_0denote the distance from center of the beam, beam radius and amplitude of electric field. The Gaussian beam plot is shown in Fig. 2(a) & Fig. 2(b). It was used as input beam (beam radius – 5 mm) to the cavity. We chose the matrix of size 128×128 and length of the grid as 0.32 m×0.32 m. The input mirror aperture was defined as shown in the Fig. 2(c). To study the mirror wave front distortion, the optical path difference (Eq. (1) and Eq. (2)) representing the mirror should also be discretized.

$$\Delta OPL(X,Y) = 2\,(R_1 - \left({R_1}^2 - (X^2 + Y^2)\right)^{1/2}) \quad \ldots (1)$$

$$\Delta r^2 = X^2 + Y^2 \quad \ldots (2)$$

R_1 and Δr represent the radius of curvature for the input mirror and distance from center of the mirror. We have used input concave mirror of R_1 = 60 cm with reflectivity 99.9 %.

The observed output from the input mirror is shown in Fig. 2(d). In next step, the field is propagated through the cavity using the plane wave equation represented as (Eq. (3)),

$$E\ (\nu_X, \nu_Y, L) = E\ (\nu_X, \nu_Y, 0)\ exp|-i[k - \pi\lambda\ \nu X2 + \nu Y2\ L \quad \ldots (3)$$

$E\ (\nu_X, \nu_Y, 0)$,k, λ, L and (ν_X, ν_Y) denote the field at zero distance, propagation vector, wavelength of laser, distance of propagation and spatial frequencies of the field[18]. The beam passes through the length of the cavity (320 mm) and observed profile of the beam is shown in Fig. 2(e). There was some distortion in the beam, due to the divergence of beam with the distance of propagation. The beam was further passed through the output mirror aperture (Fig. 2(f)) with 1.0 m radius of curvature and 99.5% reflectivity. The observed output beam could be clearly seen in the Fig. 2(g) which was of Gaussian nature as well. Therefore, we can say that the length of cavity and radius of curvature of the mirrors, we are considering for our resonator design are suitable for the formation of stable LC. To check the stability of the LC, stability analysis had been performed and obtained plot is shown in the Fig. 2(h). There is g_1 parameter on x axis and g_2 parameter on y axis of the plot. Since, the stability criterion of the optical cavity is defined by $0 \leq g_1 g_2 \leq 1$[3]. The value of g_1g_2 based on our design came ~ 0.3 which is under the bounds of the stability and shown by the red dot in the stability plot.

Using simulation, adequacy of selected parameters was checked, to form the stable resonator. Because the mirror mount movement is required at the end of cavity, for initial alignment, hence the LC rods, on which the mounts are placed, must have uniform surfaces for optimal mount movement. LC rod was characterized to ensure the surface uniformity. The linear movement of one of the mirrors is essential to vary the cavity length, deliberately to scan the frequency. For this purpose, we have designed a spline shaft to hold the mirror and to give it a translational movement. The splines need to be straight for the precise movement of the mirror, and the diameter needs to be characterized accurately to hold the mirror properly. Thus, the parameters such as spline straightness, shaft diameter and the depth of the spline need to be evaluated with utmost accuracy and precision.

3 Dimensional Characterizations of the Cavity Components

3.1 Description of Components

Our design is based on the use of three invar rods to make the system stable yet lighter and compact as compared to four invar rods. In this design, we have proposed to use the trapezoidal endplates to save the extra space gained by the rectangular/square plates. The three point mechanical system is considered as stable system for better control and stabilization. Fig. 3(a) shows the mechanical structure of cavity with three LC rods and Fig. 3(b) shows the fabricated LC rod. Invar rods were preferred for holding the mirror mounts in frequency stabilized lasers to be used for precise measurements in dimensional metrology due to the dimensional stability and low coefficient of thermal expansion (CTE) of invar as compared to other metals. Invar comprises of iron (64%) and nickel (36%) and have other scientific and industrial applications in opto mechanical engineering domains as well[19].

Mirrors should always be detained in place by appropriate mounts. The mirror mounts are attached to invar rods so that it is easy to move the mirrors while performing alignment of the cavity initially. There should be some provision to move the mirror mount at the ends of the LC rod which requires characterization of the ends of rods. The alignment is essential to minimize the loss and to increase the efficiency of the system. Further, length of cavity needs to be modulated for phase sensitive detection of absorption features. Thus, cavity design consisted of a spline shaft with four straight splines which was designed for linear guide mechanism of the mirror

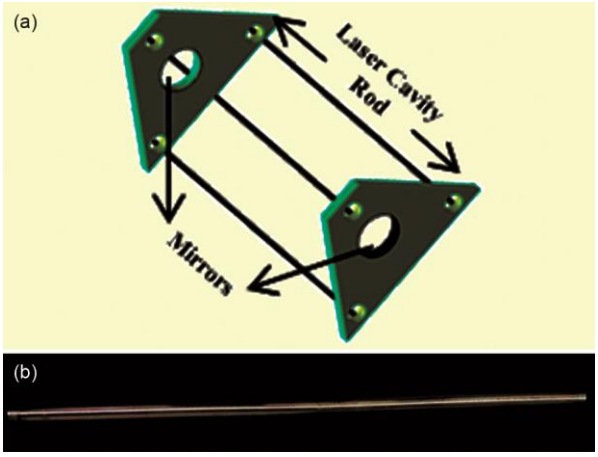

Fig. 3 — (a) Mechanical structure of laser cavity (LC) (b) Fabricated invar rod.

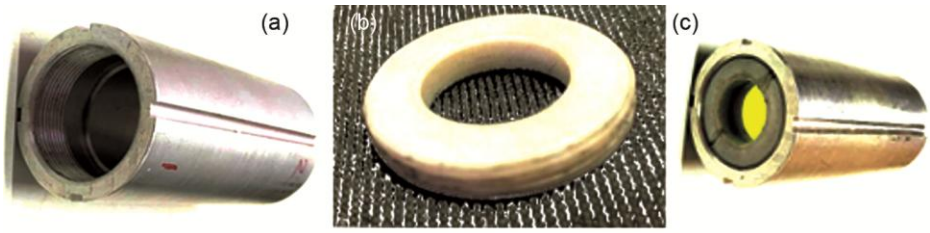

Fig. 4 — (a) Spline shaft (b) Lock nut (c) Holding of mirror in the shaft.

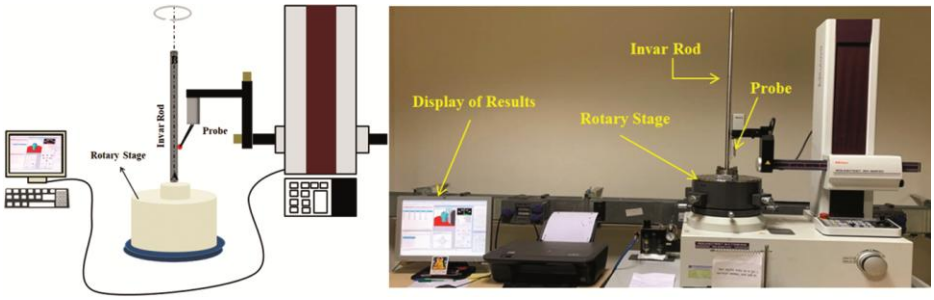

Fig. 5 — Schematic of form tester (roundness measuring machine, RA-2200 CNC) and the actual setup.

and made up of aluminum metal for the light weight consideration. Splines in the shaft are at equal distances across the diameter of the shaft. There was threading across one third part of the shaft to hold the mirror through lock nut. Fig. 4(a) to 4(c) shows fabricated spline shaft, fabricated lock nut and holding of mirror in the shaft.

3.2 Measurement Strategy and Setup

LC rod was characterized using the form tester (RA- 2200 CNC). Prior to measurements, the invar rod was cleaned and kept in recommended environmental condition of laboratory for 4 hours so that the variation in temperature and eccentricity of the form tester and measuring rod is negligible. The axis of rod was aligned with the rotational axis of the rotary table called as 'centering'. The roundness was measured at two ends of the rod marked as side A and side B using form tester. The setup comprised of a computer numerically controlled turntable/stage and probe as shown in Fig. 5. It captures the raw data and then various filters- fitting of circle is used. The ROUNDPAK software[20] collected the data and stored it in a database. The measurement data generated reference circles, to define the roundness value and least square circle (LSC) method was used to determine the roundness, by averaging all measured points on the periphery of profile. Here, the peak to valley roundness deviation, denoted as RONt, was determined as per ISO 12181-1-2011 and ISO 12181-2-2011[21, 22].

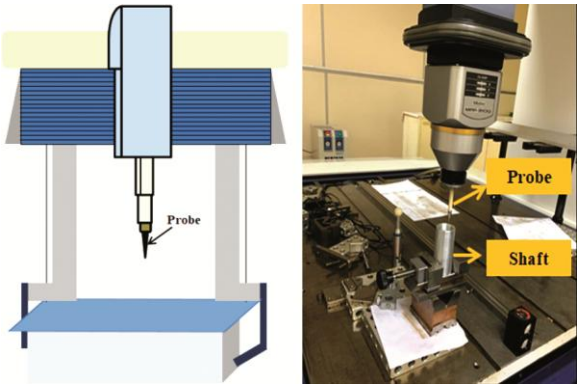

Fig. 6 — Schematic of coordinate measuring machine (CMM, LEGEX 9106) at CSIR – NPLI, and close view of the actual CMM setup.

For dimensional characterization of spline shaft, a traceable 3D-CMM (LEGEX 9106) was used; the measurement setup is shown in Fig. 6. 3D-CMM can measure the dimensions of a wide variety of artefacts[23, 24] and it measured the geometry of objects by sensing discrete points on the surface of the object using a probe. The information of discrete points based on a coordinate system determined by the equipment was recorded and further processed the coordinate values with a computer. Probe can move in X, Y and Z directions and there is a sensor that monitors the position of probe along that axis.

4 Results and Discussion

The present article discussed roundness of LC rod, measured using form tester (RA- 2200 CNC) and

dimensional characterization of spline shaft conducted using 3D-CMM. These parameters are needed to be accurately determined for the design and development of dimensionally stable resonator.

4.1. Roundness of LC Rod

Nine set of observations were taken for a single set of revolution of the rotary stage as given in Table 2. Fig. 7 depicts the observed profiles. Deviation in roundness was calculated on the basis of LSC and associated filter undulations per revolution (UPR). Model function for the measured value can be formulated as given in Eq. (4),

$$\text{Measured Value} = \delta_s + \delta_{ft} + \delta_{ecc} + \delta_{rep} \quad \ldots (4)$$

Where, δ_s denote the correction due to hemisphere standard, δ_{ft} correction due to resolution of form tester, δ_{ecc} correction due to eccentricity of form tester and δ_{rep} correction due to observed measurements. For uncertainty evaluation GUM/LPU approach was used and the detailed uncertainty budget as per LPU is given in Table 3.

Lesser the roundness error, longer the bearing life which is useful for precise linear movement applications. Therefore, the rods fitted well within the desired range that ensures the optimal mount movement and dimensional stability of the laser system.

Table 2 — Observation table for roundness measurement of LC rod Temperature = 20.5 ℃ , Relative humidity = 54.6 %

S. No.	Roundness (μm)		
	Side A	Side B	Filter used: Gaussian 50 %, 50 UPR
1	2.973	1.069	
2	2.974	1.064	
3	2.982	1.071	
4	2.972	1.063	
5	2.962	1.072	
6	2.973	1.082	
7	2.956	1.075	
8	2.959	1.081	
9	2.961	1.079	
Average Roundness	2.968	1.073	
Maximum Roundness	2.982	1.082	
Standard Deviation	0.0087	0.0069	
Type A uncertainty	0.0029	0.0023	

4.2. Characterization of Spline Shaft

Table 4 shows the observations for inner diameter and outer diameter measurement of the spline shaft (80 mm length, L) along with straightness & depth of spline.

Model function for the measured value can be formulated as given in Eq. (5),

$$\text{Measured Value} = \delta_s + \delta_{pb} + \delta_t + \delta_\alpha + \delta_{pbr} + \delta_{gmr} + \delta_{rep} \quad \ldots (5)$$

Where, $\delta_s$denote the correction due to standard, δ_{pb} correction due to the resolution of probe, δ_t correction due to variation in the temperature, δ_α correction due to the variation in coefficient of thermal expansion, δ_{pbr} correction due to the probing error while taking measurements, δ_{gmr} correction due to the geometrical error which include the alignment errors and δ_{rep} correction due to repeatability.

The observed profile for diameter measurement is shown in Fig. 8 and Table 5 shows the uncertainty budget as per GUM/LPU for spline shaft measurements. While measuring the point to point measurements, if one end of the shaft is labeled as A and the other one as B, then the measurement sequence is either A_1B_1, A_2B_2, A_3B_3 or A_1B_1, B_2A_2, A_3B_3.

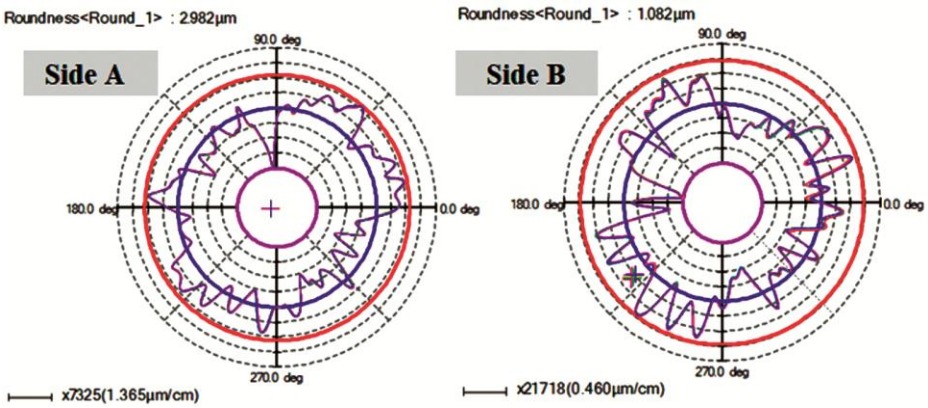

Fig. 7 — Roundness profiles.

Table 3 — Uncertainty budget as per LPU for roundness measurement of LC rod

Sources of Uncertainty	Estimate (±) in μm	Probability Distribution	Standard Uncertainty	Sensitivity Coefficient	Degree of freedom	Uncertainty Contribution
Associated uncertainty of hemisphere standard	0.009	Normal,B	0.0045	1	∞	± 0.0045
Form Tester Resolution	0.001	Rectangular, B	0.0006	1	∞	± 0.0006
Eccentricity of form tester	0.009	Rectangular, B	0.0040	1	∞	± 0.0040
Repeatability, Side A	2.968	Normal,A	0.0029	1	8	± 0.0029
Repeatability, Side B	1.073	Normal,A	0.0023	1	8	± 0.0023
		Combined Uncertainty (k=1), Side A				± 0.0067 μm
		Combined Uncertainty (k=1), Side B				± 0.0065 μm
		Expanded Uncertainty (k=2), Side A				± 0.0134 μm
		Expanded Uncertainty (k=2), Side B				± 0.0130 μm

Table 4 — Observations for spline shaft measurements Temperature = 19.8 ℃ , Relative humidity = 57 %

S.No.	Diameter (mm)			Straightness (mm)	Depth of the spline
	Inner Diameter	Outer Diameter			Distance x (mm)
		Side A	Side B		
1.	25.5183	35.0313	35.0936	2.5688	15.9852
2.	25.5225	35.0315	35.096	2.4948	15.9857
3.	25.5178	35.0317	35.0957	2.5258	15.9857
4.	25.5193	35.0313	35.0946		
5.	25.5147	35.0314	35.0916		
Mean	25.5185	35.03144	35.0943	2.5298	15.98553
Standard Deviation	0.0028	0.000167	0.001783	0.037162	0.000289
Standard Uncertainty	0.0013	7.48×10^{-5}	7.97×10^{-3}	0.021455	0.000167

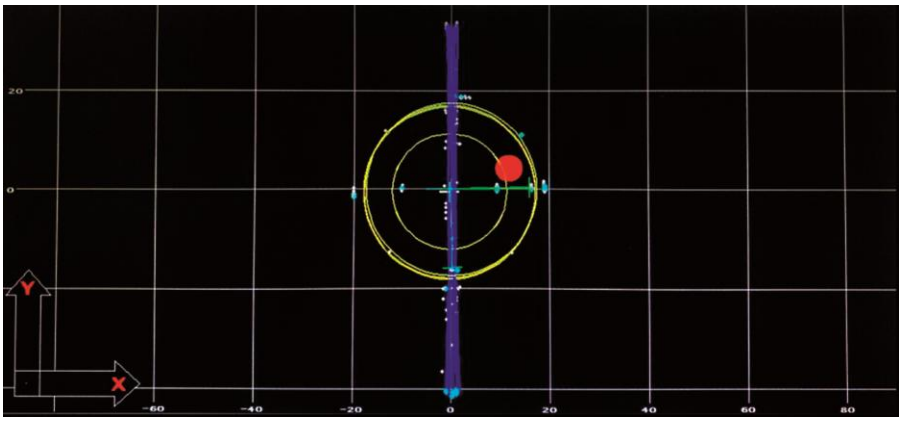

Fig. 8 — Observed profile.

To determine the depth of the spline, the distance x had been measured using the probe of CMM (Fig. 9). Outer diameter of the shaft is already known. Using the formula given in Eq. (6), depth of spline can be obtained.

$$y = \text{Radius of shaft} - \text{Distance (x)} \quad \ldots (6)$$

The dimensional parameters of a spline shaft, namely the inner diameter of the shaft, the outer diameter of the shaft, the straightness of the spline, and the depth of the spline, were measured via point-to-point measurements on the shaft's surface. These parameters could be used to determine whether the geometrical form of the manufactured shaft meets the specified requirements such as the splines are straight enough for precise translation of mirror to change the cavity length and the diameter of shaft to ensure the perfect holding of mirror to reduce the error during fine adjustment of mirror. Spline shaft is proposed to be attached by a spline hub which also consists of

Table 5 — Uncertainty budget as per LPU for spline shaft measurements

Sources of error			Limits (±)	Probability distribution	Standard uncertainty (μm)	Sensitivity coefficient	Uncertainty Contribution	
							Length Independent	Length Dependent
Associated Uncertainty of standard (μm)			0.36	Normal, B	0.18	1	± 0.18	-
Resolution of probe (μm)			0.01	Rectangular, B	0.006	1	± 0.006	-
Temperature variation (℃)			1	Rectangular, B	0.577	$2.3 \times 10^{-5} \times L$	-	$\pm 1.327 \times 10^{-5} \times L$
Variation in coefficient of thermal expansion ($℃^{-1}$)			0.23×10^{-5}	Rectangular, B	0.1328×10^{-5}	$0.36\times L$	-	$\pm 0.048 \times 10^{-5} \times L$
Probing error (μm)			5	Rectangular, B	2.887	1	± 2.887	-
Geometrical error (μm)			0.2	Rectangular, B	0.115	1	± 0.115	-
Repeatability (mm)	Inner Diameter		25.5185	Normal, A	1.3	1	± 1.3	-
	Outer Diameter	Side A	35.03144	Normal, A	0.0748	1	± 0.0748	-
		Side B	35.0943	Normal, A	7.97	1	± 7.97	-
	Straightness of Spline		2.5298	Normal, A	21.45	1	± 21.45	-
	Depth of Spline	Distance x	15.98553	Normal, A	0.167	1	± 0.167	-
Combined uncertainty u_c (k=1) (μm)				Inner diameter			± 3.173	
				Outer diameter (Side A)			± 2.895	$\pm 1.328\times 10^{-5} \times L$
				Outer diameter (Side B)			± 8.479	
				Straightness of spline			± 21.644	
				Depth of spline (Distance x)			± 2.899	
Expanded uncertainty (k=2) (μm)				Inner diameter			± 6.346	
				Outer diameter (Side A)			± 5.790	$\pm 2.656\times 10^{-5} \times L$
				Outer diameter (Side B)			± 16.958	
				Straightness of spline			± 43.288	
				Depth of spline (Distance x)			± 5.798	

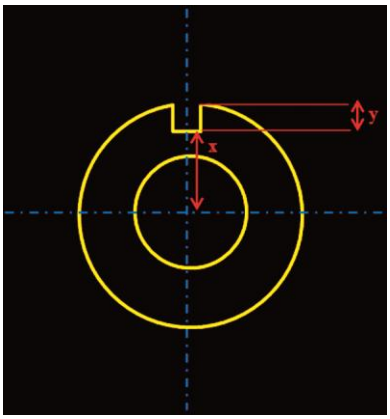

Fig. 9 — Depth measurement.

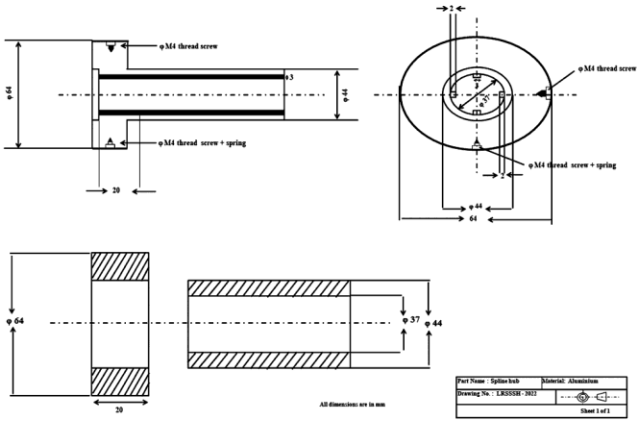

Fig.10 — Mechanical drawing for the spline hub.

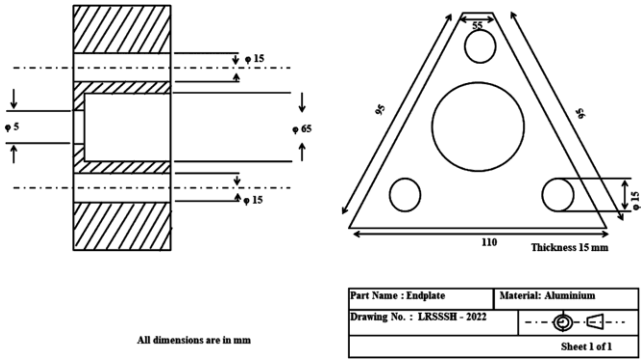

Fig. 11 — Mechanical drawing for the endplates.

four solid splines as shown in Fig. 10 and it is attached to the endplate as shown in Fig. 11. These are the proposed design for the complete mirror mounts and their holding in the laser cavity. The shaft would be moved with the help of piezoelectric transducer.

5 Conclusion

Initially, the length of cavity was estimated of 320 mm length and appropriateness of the selected length and stability analysis was carried out using octave software. Simulation shows that the parameters selected were appropriate to design a stable resonator. Furthermore, the fabricated resonator components *i.e.* LC rod for mirror mount movement during the initial alignment of cavity and spline shaft for precise

holding and translation of one of the mirrors to change the cavity length in order to scan the frequency, were characterized. The characterization of cavity components has been carried out using form tester (RA- 2200 CNC) and 3D coordinate measuring machine (3D-CMM, LEGEX 9106). At side A of LC rod, the roundness was (2.982 ± 0.0134) μm and for side B, roundness was (1.082 ± 0.0130) μm. The uncertainty was obtained using ISO GUM/LPU approach.Lower the roundness uncertainty, even the surface quality, which is useful for precise linear movement applications. The spline shaft was characterized using 3D-CMM. The observed inner diameter of the shaft was (25.5185 ± 0.0063) mm. Since, the other side of the shaft was threaded for holding the mirror, the inner diameter was only measured on one side of the shaft. The outer diameter observed was (35.03144 ± 0.0058) mm at one end and (35.0943 ± 0.0170) mm at the other. The straightness of the splines measured showed uncertainty of 0.0433 mm and the depth of the spline was (1.5301 ± 0.0058) mm. The outcomes revealed that the designed shaft is adequate for holding the mirror and splines straightness is suitable for the precise movement of mirror to vary the cavity length. Therefore, we may infer that the fabricated parts fulfil the requirements for the development of a stable resonator.

Acknowledgements

The authors are thankful to Director, CSIR-National Physical Laboratory (NPL, India) for constant encouragement and support. One of the authors, Anju, would like to thank Council of Scientific and Industrial Research (CSIR) for fellowship. The authors also would like to thank Mr. Jokhan Ram, Mr. Vinod Kumar and Mr. Sandeep Kumar for the technical support. The authors are also thankful to the central workshop at CSIR – NPL for helping in the fabrication of components.

References

1 Svelto O and David C H, *Principles of lasers*, New York: Plenum press, 4 (1998).
2 Silfvast W T, *Laser fundamentals*, Cambridge University Press, 2004.
3 Siegman A E, *Lasers*, University science books, 1986.
4 Hecht J, Laser Characteristics, in Understanding Lasers: An Entry-Level Guide, *IEEE*, (2019) 95-126, doi: 10.1002/9781119310693.ch4.
5 Leonhardt V & Jordan B C, *Appl Opt*, 45 (2006) 4142.
6 Brand U, *Opt Commun*, 100 (1993) 361.
7 Saptari V, *Fourier transform spectroscopy instrumentation engineering*, Bellingham Washington, DC: SPIE Optical Engineering Press, 2003.
8 Cerez P, Brillet A, Man-Pichot C & Umezu J, *Academie des Sciences Paris Comptes Rendus Serie B Sciences Physiques*, 290 (1980) 515.
9 El-Hennawi H, Mohamed S, Mohamed A & Osama T, Two-Mode Frequency Stabilization of an Internal Mirror 633nm He-Ne Laser, In 10th IMEKO TC7 International Symposium, Saint-Petersburg, Russia, (2004) 412.
10 Baer T, Kowalski F V & John L H, *Appl Opt* 19 (1980) 3173.
11 Bertinetto F P, Cordiale S F & Picotto G B. *IEEE Trans Instrum Meas*, 2 (1985) 256.
12 Riehle F, Patrick G, Felicitas A & Lennart R, *Metrologia*, 55 (2018) 188.
13 JCGM 100:2008 – Evaluation of measurement data – Guide to the expression of uncertainty in measurement, Joint Committee for Guides in Metrology; 2008.
14 Joint Committee for Guides in Metrology (JCGM), JCGM 101: 2008. Evaluation of measurement data—Supplement 1 to the Guide to the expression of uncertainty in measurement—Propagation of distributions using a Monte Carlo method. (2008).
15 JCGM 102: 2011, Evaluation of measurement data– Supplement 2 to the Guide to the expression of uncertainty in measurement – Extension to any number of output quantities, (2011).
16 Anju, Moona G, Jewariya M, Arora P & Sharma R, *MAPAN*, 36 (2021) 467.
17 Singari R M & Kankar P K, *Adv Prod Indus Eng Proc of ICAPIE*, 27 (2022) 462.
18 Degallaix J, *Software X*, 12 (2020) 100587.
19 Sahoo A & Medicherla V R R, *Mater Today*, 43 (2021) 2242.
20 https://www.mitutoyo.com/Images/ra-tradein.pdf
21 ISO 12181-1:2011, Geometrical product specifications (GPS), Roundness, Part 1: Vocabulary and parameters of roundness.
22 ISO 12181-2:2011, Geometrical product specifications (GPS), Roundness, Part 2: Specification operators.
23 Moona G, Kumar V, Jewariya M, Kumar H & Sharma R, *The Int J Adv Manuf Technol*, 119 (2022) 5903.
24 Altinisik A & Emre B, *Measurement*, 168 (2021) 108228.